Electronic Supplementary Material (ESI) for Journal of Materials Chemistry A.

Sn-stabilized Li-rich layered $Li(Li_{0.17}Ni_{0.25}Mn_{0.58})O_2$ oxide as cathode for advanced lithium-ion batteries

Qi-Qi Qiao, Lei Qin, Guo-Ran Li, Yong-Long Wang and Xue-Ping Gao*

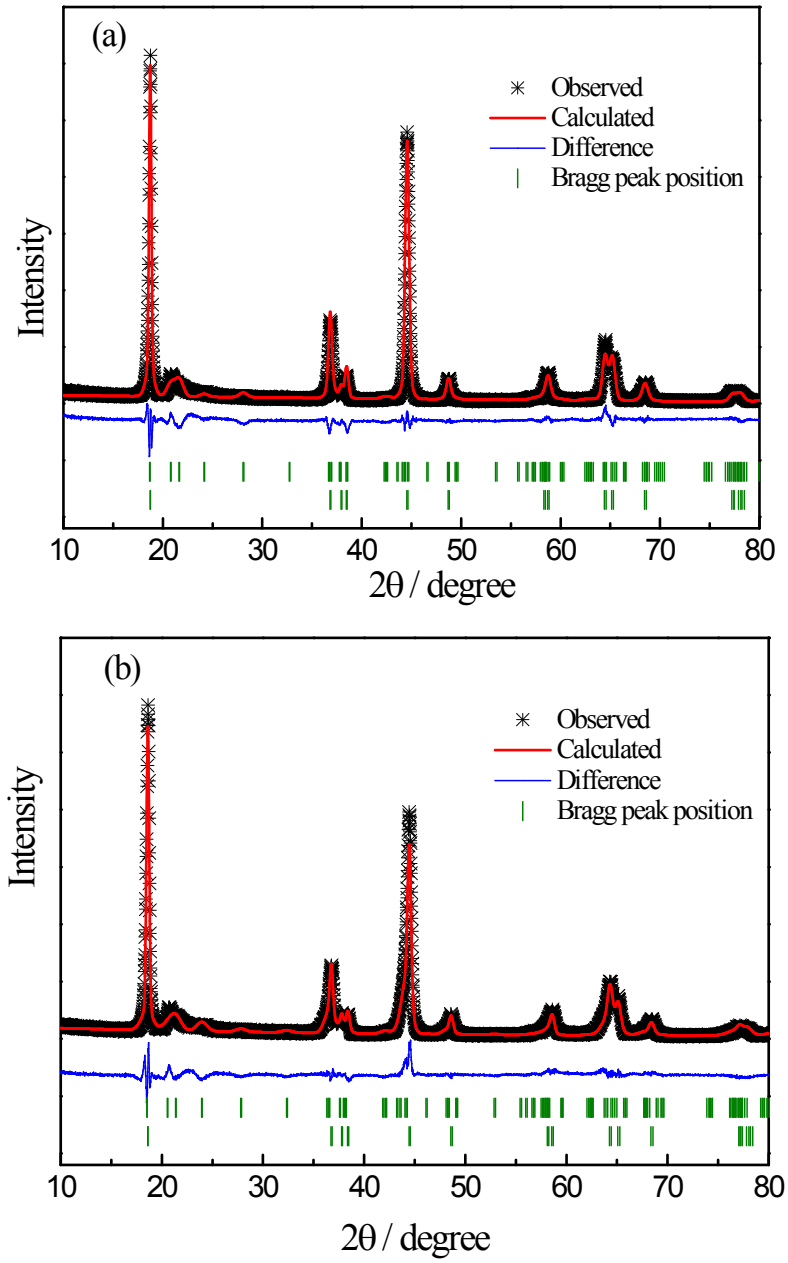

Fig. S1. Reitveld refinements of the pristine LNMO (a) and LNMO-$Sn_{0.01}$ (b) based on the $LiNi_{0.5}Mn_{0.5}O_2$ ($R\bar{3}m$) and Li_2MnO_3 (C2/m) structure. $Li_{1.17}Ni_{0.25}Mn_{0.58}O_2$ is considered as $0.4Li_2MnO_3 \cdot 0.6LiNi_{0.5}Mn_{0.5}O_2$, while $Li_{1.17}Ni_{0.25}Mn_{0.57}Sn_{0.01}O_2$ is considered as $0.4Li_2Mn_{0.98}Sn_{0.02}O_3 \cdot 0.6LiNi_{0.5}Mn_{0.49}Sn_{0.01}O_2$. Here, the occupancy of Sn site is set to replace Mn site to refine.

Table S1. The atom parameters for $LiNi_{0.5}Mn_{0.5}O_2$ phase in LNMO and LNMO-$Sn_{0.01}$ materials. sg = space group, occ = site occupancy.

sg: $R\bar{3}m$	LNMO				LNMO-$Sn_{0.01}$			
	x	y	z	occ	x	y	z	occ
Li (3a)	0	0	0	0.913(6)	0	0	0	0.928(6)
Li (3b)	0	0	0.5	0.086(4)	0	0	0.5	0.071(4)
Ni (3a)	0	0	0	0.086(4)	0	0	0	0.071(4)
Ni (3b)	0	0	0.5	0.414(4)	0	0	0.5	0.429(4)
Mn (3b)	0	0	0.5	0.5000	0	0	0.5	0.49000
Sn (3b)					0	0	0.5	0.01
O (6c)	0	0	0.2437(7)	1	0	0	0.241407	1

Table S2. The atom parameters for Li_2MnO_3 phase in LNMO and LNMO-$Sn_{0.01}$ materials. sg = space group, occ = site occupancy.

sg: C2/m	LNMO				LNMO-$Sn_{0.01}$			
	x	y	z	occ	x	y	z	occ
Li (2b)	0	0.5	0	1	0	0.5	0	1
Li (2c)	0	0	0.5	1	0	0	0.5	1
Li (4h)	0	0.6606	0.5	1	0	0.6606	0.5	1
Mn (4g)	0	0.1668(6)	0	1	0	0.1667(8)	0	0.98
Sn (4g)					0	0.1667(8)	0	0.02
O (4i)	0.2098(17)	0	0.2412(23)	1	0.2722(18)	0	0.2262(21)	1
O (8j)	0.2160(19)	0.3425(8)	0.2379(27)	1	0.2853(20)	0.3346(9)	0.2654(20)	1

Table S3. Summary of the *R* factors and the crystallographic parameters for LNMO and LNMO-$Sn_{0.01}$ materials

	Rwp (%)	Rp (%)	Cell parameters (Å)			Ni in Li layer (%)
			a	b	c	
LNMO	12.7	11.2	2.86221(22)	2.86221(22)	14.2387(23)	8.6
Li_2MnO_3 in LNMO			4.9573(15)	8.598(4)	5.0262(24)	
LNMO-$Sn_{0.01}$	12.6	10.9	2.86179(23)		14.2642(25)	7.1
Li_2MnO_3 in LNMO-$Sn_{0.01}$			5.0042(35)	8.633(5)	5.0631(30)	

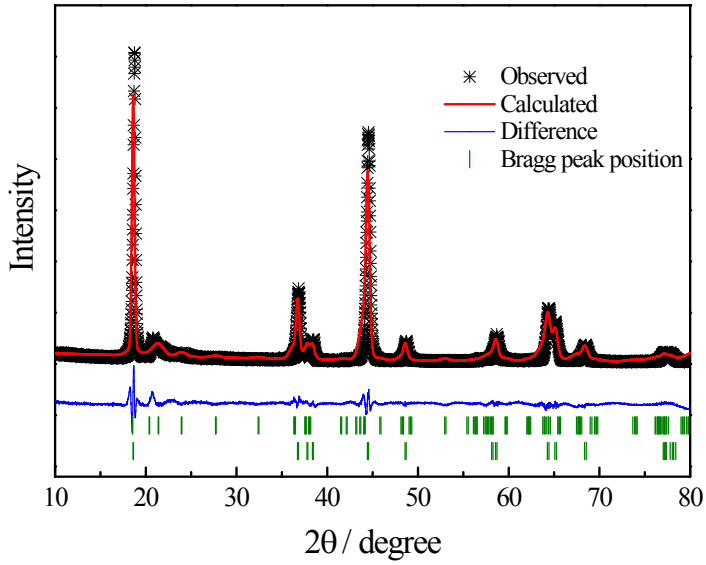

Fig. S2. Reitveld refinements of the pristine LNMO (a) and LNMO-$Sn_{0.01}$ (b) based on the $LiNi_{0.5}Mn_{0.5}O_2$ ($R\bar{3}m$) and Li_2MnO_3 (C2/m) structure. Here, the occupancies of Sn and Mn free to refine.

Table S4. The atom parameters for $LiNi_{0.5}Mn_{0.5}O_2$ phase in LNMO-$Sn_{0.01}$ material. sg = space group, occ = site occupancy.

sg: $R\bar{3}m$	LNMO-$Sn_{0.01}$			
	x	y	z	occ
Li (3a)	0	0	0	0.969(6)
Li (3b)	0	0	0.5	0.031(6)
Ni (3a)	0	0	0	0.031(6)
Ni (3b)	0	0	0.5	0.469(6)
Mn (3b)	0	0	0.5	0.649(13)
Sn (3b)	0	0	0.5	-0.149(13)
O (6c)	0	0	0.241407	1

Table S5. The atom parameters for Li_2MnO_3 phase in LNMO-$Sn_{0.01}$ material. sg = space group, occ = site occupancy.

sg: C2/m	LNMO-$Sn_{0.01}$			
	x	y	z	occ
Li (2b)	0	0.5	0	1
Li (2c)	0	0	0.5	1
Li (4h)	0	0.6606	0.5	1
Mn (4g)	0	0.1585(10)	0	1.492(9)
Sn (4g)	0	0.1585(10)	0	-0.492(9)
O (4i)	0.2347(21)	0	0.2503(25)	1
O (8j)	0.3095(22)	0.3277(11)	0.2359(21)	1

Table S6. Summary of the *R* factors and the crystallographic parameters for LNMO-$Sn_{0.01}$ material

	Rwp (%)	Rp (%)	Cell parameters (Å)		
			a	b	c
LNMO-$Sn_{0.01}$	11.9	9.6	2.86171(25)		14.2615(29)
Li_2MnO_3 in LNMO-$Sn_{0.01}$			4.9980(30)	8.689(5)	5.0607(35)

As shown in **Table S1, S2,** and **S3**, the refinement is acceptable with a low Rp value. When the occupancies of Sn and Mn are free to replace in the refinement, it is not appropriate with the appearance of negative occupancy (**Fig. S2 and Table S4, S5**). It means that the occupancy of Sn atoms on Mn positions in the layered structure is reasonable.

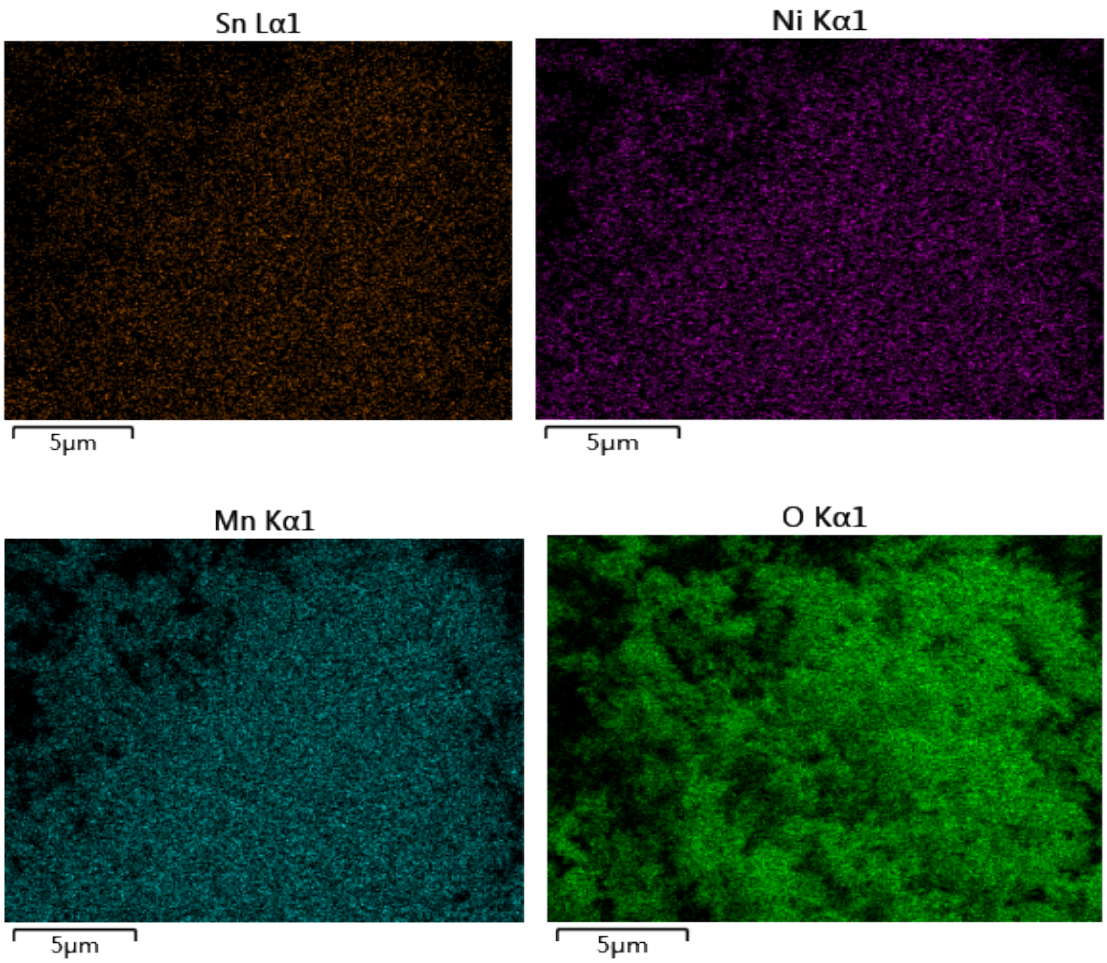

Fig. S3. The EDS mappings of Sn, Ni, Mn, and O in the LNMO-$Sn_{0.03}$ samples.

Table S7. Element concentration obtained by ICP-MS (wt%)

	Li	Ni	Mn	Sn
LNMO	9.72	15.9	32.6	
LNMO-$Sn_{0.03}$	9.08	15.9	29.8	2.26

Table S8. Atomic ratio based on ICP-MS

	Li	Ni	Mn	Sn
LNMO	1.21	0.24	0.51	
LNMO-$Sn_{0.03}$	1.16	0.24	0.48	0.02

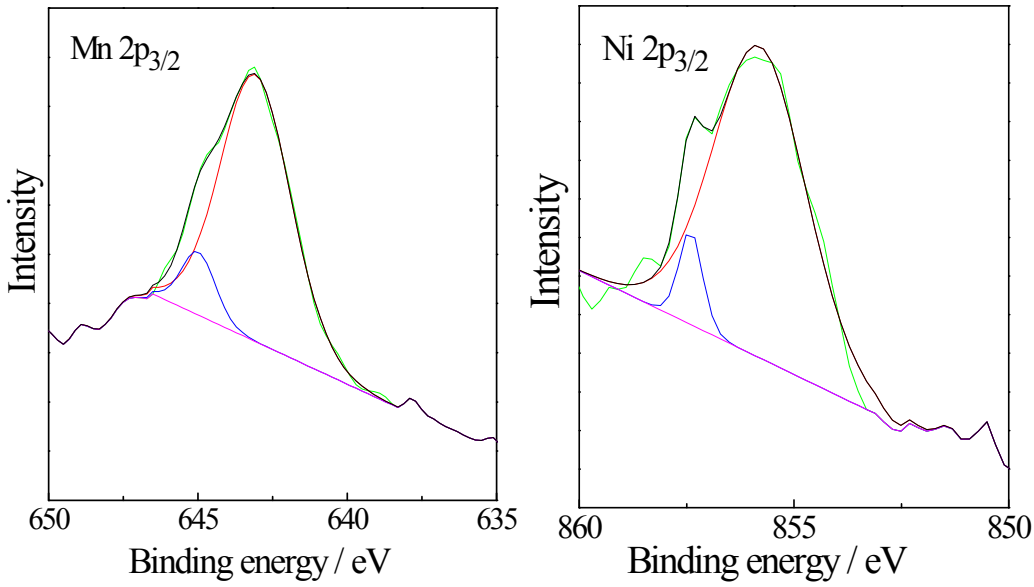

Fig. S4. XPS spectra and fitted curves of the LNMO-$Sn_{0.03}$ samples: Mn 2p and Ni 2p core levels.

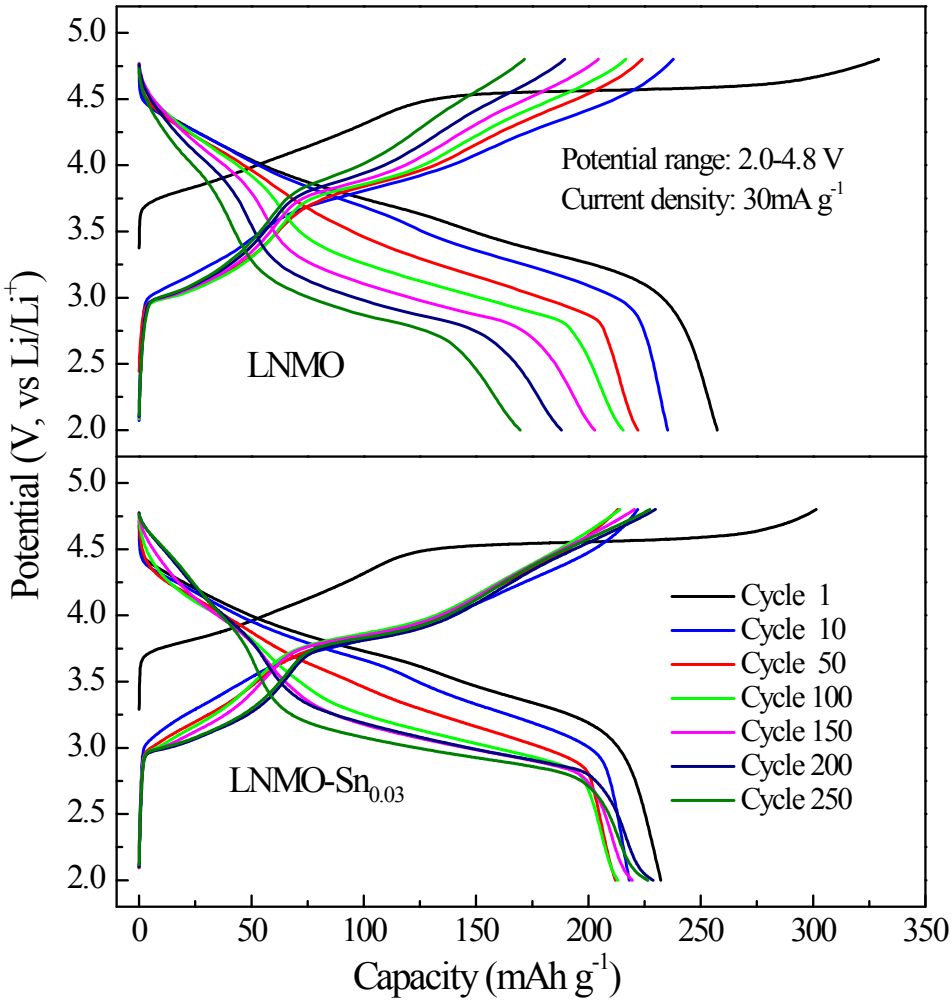

Fig. S5. The charge–discharge curves of the LNMO and LNMO-$Sn_{0.03}$ samples in different cycles at 0.1 C rate (30 mA g^{-1}) between 2.0 and 4.8 V (vs Li/Li^+)

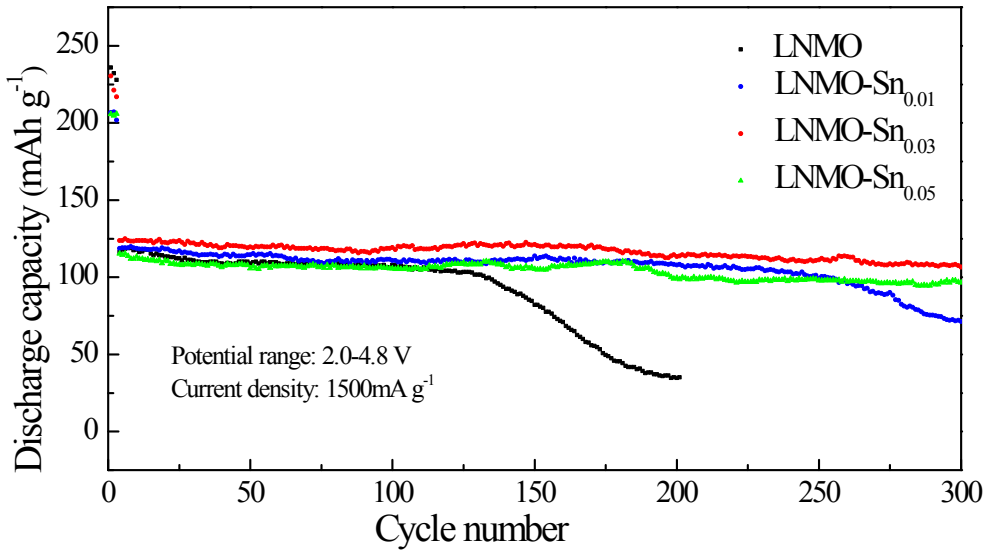

Fig. S6. Cycle performances of LNMO, LNMO-$Sn_{0.01}$, LNMO-$Sn_{0.03}$, and LNMO-$Sn_{0.05}$ samples at 5 C rate (1500 mA g^{-1})

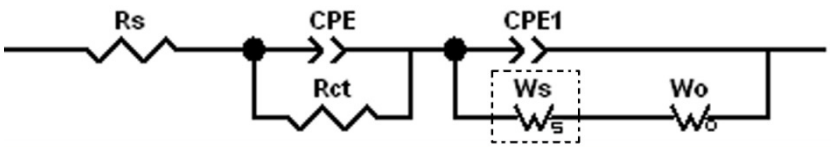

Fig. S7. Equivalent circuits used to fit the experimental data. R_s is solution resistance, R_{ct} is charge-transfer resistance, CPE and CPE1 are constant phase element, W_s and W_o are assigned to the finite Nernst diffusion impedance in the thin film and semi-infinite Warburg diffusion impedance in the bulk, respectively.

Table S9. The simulated results from electrochemical impedance spectra of the $Li(Li_{0.17}Ni_{0.25}Mn_{0.58})O_2$ and Sn^{4+} substituted samples.

Sample	Cycle	R_{ct} (Ω)	W_s (Ω)	W_o (Ω)
$Li(Li_{0.17}Ni_{0.25}Mn_{0.58})O_2$	1st	471.9	-	411.3
	10th	38.1	-	9013
	30th	43.6	-	9508
	50th	43.9	1029	2503
	100th	44.6	628	2862
$Li(Li_{0.17}Ni_{0.25}Mn_{0.57}Sn_{0.01})O_2$	1st	359.1	397.4	2991
	10th	72.3	940.2	1316
	30th	68.8	524.2	875
	50th	81.2	1173	1145
	100th	91.1	791.9	1231
$Li(Li_{0.17}Ni_{0.25}Mn_{0.55}Sn_{0.03})O_2$	1st	262.6	398.6	951
	10th	56.2	1334	1801
	30th	78.3	1338	1809
	50th	97.7	454.1	1258
	100th	155.8	1189	1352
$Li(Li_{0.17}Ni_{0.25}Mn_{0.53}Sn_{0.05})O_2$	1st	188.0	1768	1299
	10th	43.5	639.1	523.8
	30th	33.4	874.2	1388
	50th	30.8	905.8	1887
	100th	41.9	962.5	1322